Image observations in data assimilation

F.X. Le Dimet, **I. Souopgui**, O. Titaud, A. Vidard

Team - project INRIA MOISE

French Research Agency project ADDISA

Laboratoire Jean Kuntzmann, Grenoble, France

http://addisa.gforge.inria.fr

ADAMS meeting, Paris, october 29, 2009

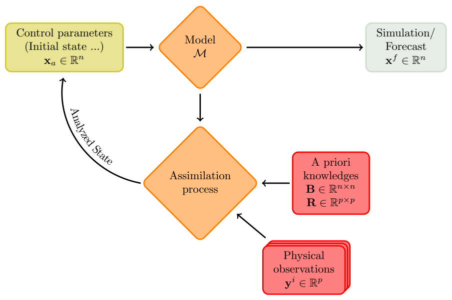

- Forecast is produced by integration of a model from an initial state

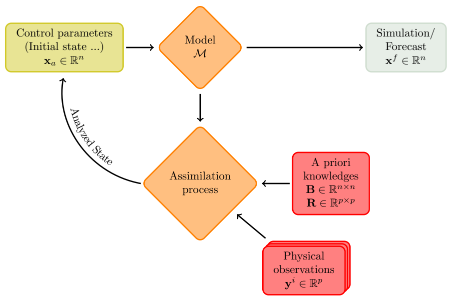

- Forecast is produced by integration of a model from an initial state
- Data Assimilation combines in a coherent manner all the available informations in order to retrieve an optimal initial state and then perform a forecast:
  - Mathematical and physical information : model
  - In-situ and remote measurements of the true state
  - A priori knowledges (background, errors . . .)

The state of the flow is governed by a partial differential system

$$\left\{ \begin{array}{rcl} \dfrac{\partial \mathbf{X}}{\partial t} & = & \mathcal{M}(\mathbf{X}) \\ \mathbf{X}(0) & = & \mathbf{U} \end{array} \right.$$

U : initial state

Cost function

$$J(\mathbf{X_0}) = \frac{1}{2}\int_0^T \|\mathcal{H}[\mathbf{X}] - \mathbf{Y}^o\|_{\mathcal{O}}^2 + \frac{1}{2}\|\mathbf{X_0} - \mathbf{X^b}\|_{\mathcal{X}}^2$$

Adjoint (backward) model

$$\left\{ \begin{array}{rcl} \dfrac{\partial \mathbf{P}}{\partial t} + \left[\dfrac{\partial \mathcal{M}}{\partial \mathbf{X}}\right]^T .\mathbf{P} & = & \left[\dfrac{\partial \mathcal{H}}{\partial \mathbf{X}}\right]^T .(\mathcal{H}[\mathbf{X}] - \mathbf{y}_{obs}) \\ \mathbf{P}(T) & = & 0 \end{array} \right.$$

- Structure's dynamic into MÉTÉOSAT images (visible channel)

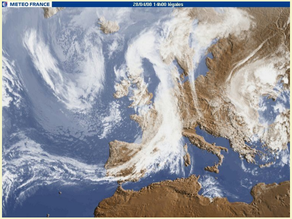

April 28, 2008, 14H00

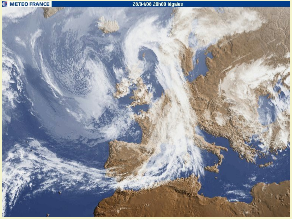

April 28, 2008, 20h00

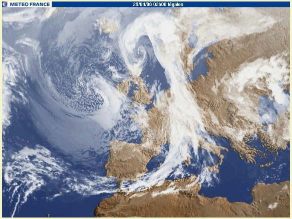

April 29, 2008, 02H00

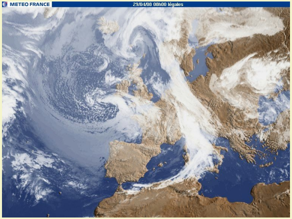

April 28, 2008, 08h00

Source : Meteo France

- Evolution of a Dry Intrusion

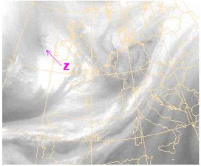

Fig 3.6(a). 19 December 1998 at 1200 UTC, also indicated 'Z' the expanding dark zone.

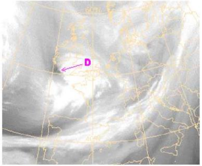

Fig 3.6(b). 19 December 1998 at 1800 UTC, also indicated 'D' the dark slot.

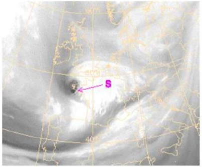

Fig 3.6(c). 20 December 1998 at 0000 UTC, also indicated 'S' the dark slot.

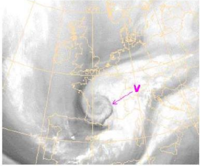

Fig 3.6(d). 20 December 1998 at 1200 UTC, also indicated 'V' the dark spiral.

- Water Vapor Canal (MÉTÉOSAT)
- Evolution of a Dry Intrusion (24 hours)
- From a common anomaly to a cyclogenesis

(Santurette and Georgiev, 2005)

Image observations : satellite images

- Satellite image sequences provide
  - A large amount of High Resolution data, (available where other sources are not)
  - A global cover of the system (geostationary satellites)
  - The evolution of some structures such as vortices, eddies, fronts or filaments
  - Informations on genesis and evolution of Extreme Events (Tropical cyclone, Hurricanes, ...)
- Currently, images and sequences of images are underused (specialist's interpretations and pseudo-observations)
  - Satellite measurements are expensive
- Application fields : Meteorology, oceanography, atmospheric sciences, hydrology, glaciology, astrophysics, medicine,. . .

Images in DA : Pseudo observations technique

Velocity fields can be estimated by some motion estimation techniques (e.g. optical flow, AMV, image model, . . .) from sequences of images

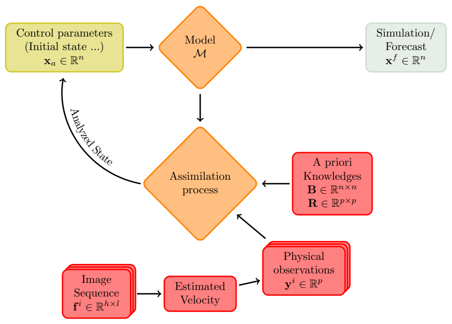

- Estimated velocity fields may be used as observations
- Pseudo-obs. transforms Lagrangian informations into Eulerian informations

(G. Korotaev, E. Huot *et al.*, 2008), (D. Auroux and M. Masmoudi, 2006), (B. Horn and B. Schunck, 1981)

Image sequences are assimilated into the Optimality System

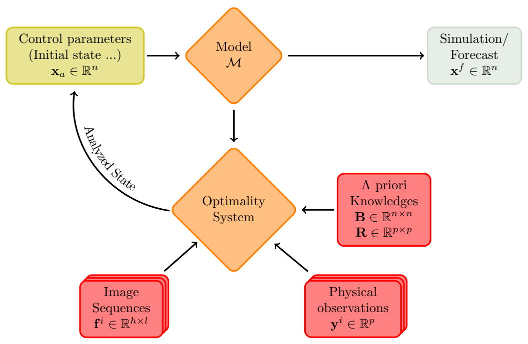

- Pseudo physical observations are avoided

Cost function : $J(\mathbf{X_0}) =$

$$\underbrace{\frac{1}{2}\int_0^T \|\mathcal{H}[\mathbf{X}] - \mathbf{Y}^o\|^2_{\mathcal{O}} dt + \frac{1}{2}\|\mathbf{X_0} - \mathbf{X^b}\|^2_{\mathcal{X}}}_{\text{classical cost function } J_o} + \underbrace{\frac{1}{2}\int_0^T \|\mathcal{H}_{\mathcal{S}}[\mathbf{X}] - \mathbf{Y}^{I_S}\|^2_{\mathcal{S}} dt}_{\text{image cost function } J_I}$$

Challenge : define/choose pertinent

- image space $\mathcal{S}$ with norm $\|.\|_{\mathcal{S}}$
- image observation $\mathbf{Y}^{I_S}$
- image observation operator $\mathcal{H}_{\mathcal{S}}$

Cost function : $J(\mathbf{X_0}) =$

$$\underbrace{\frac{1}{2}\int_0^T \|\mathcal{H}[\mathbf{X}] - \mathbf{Y}^o\|_{\mathcal{O}}^2 dt + \frac{1}{2}\|\mathbf{X_0} - \mathbf{X^b}\|_{\mathcal{X}}^2}_{\text{classical cost function } J_o} + \underbrace{\frac{1}{2}\int_0^T \|\mathcal{H}_{\mathcal{S}}[\mathbf{X}] - \mathbf{Y}^{I_S}\|_{\mathcal{S}}^2 dt}_{\text{image cost function } J_I}$$

Challenge : define/choose pertinent

- image space $\mathcal{S}$ with norm $\|.\|_{\mathcal{S}}$
- image observation $\mathbf{Y}^{I_S}$
- image observation operator $\mathcal{H}_{\mathcal{S}}$

Images are :

- indirect observation of the system(atmosphere/sea) state
  $\Rightarrow$ IR radiation for satellite images
- 2D "projection" of the 3D system

Image sequence, dynamic information

- avalaible only on edges (discontinuities)
- undefined in homogeneous area
- unavalaible along edges

$\Rightarrow$ regularization functions

- Interpretation levels
  - Pixel (low) level : unstructured information, depends a lot on the underlying physical processes, strong error correlation between pixels
  - Analysis (high) level: structured information, less depends on the underlying physics, information dominated by the dynamics

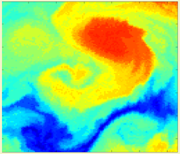

MODIS Black Sea Infrared Image (temperature)

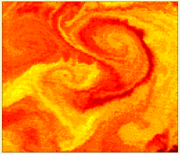

MODIS Black Sea Optical Image (ocean color)

- Mathematical framework

  multi-scale decomposition (*wavelets*, *curvelets*,...) - Partial Differential Equation framework - Stochastic approach
- Image sequences : may be considered as a 3 dimentional data

Proposition : define

- high level (well-suited to images charateristics) space $\mathcal{S}$ for images and image sequences observation cost function
- adequate image operators $\mathcal{H}_{\mathcal{F}\to\mathcal{S}}$ that map classical image space to the new one
- image observation operator $\mathcal{H}_{\mathcal{S}} = \mathcal{H}_{\mathcal{X}\to\mathcal{S}}$ that map state variables to the new space

Application

- $\mathcal{S}$: multi-scale (basis of $\mathbb{R}^2$) space; wavelets, curvelets, $\cdots$
- image operators : multi-scale decompositions
- $\mathcal{H}_{\mathcal{S}}$: two ways
  - considering image as passive tracer evolvind under the system dynamic $\mathcal{H}_{\mathcal{S}} = \mathcal{H}_{\mathcal{X}\to\mathcal{V}} \circ \mathcal{H}_{\mathcal{F}\to\mathcal{S}}$
  - modelling radiative transfert / underlying observations direct operator $\mathcal{H}_{\mathcal{S}} = \mathcal{H}_{\mathcal{X}\to\mathcal{S}}$

satellite images = IR radiation measured by satellites.
signals are well described in terms of frequential characteristics

- fourier transform for global study of the signal
- (limited-support) multi-scale transform for global and local study
  - wavelet (and is isotropic 2D adaption) well-suited for 1D signal analysis
  - curvelet (anisotropic 2D decomposition) well-suited for 2D signals

satellite images = IR radiation measured by satellites.
signals are well described in terms of frequential characteristics

- fourier transform for global study of the signal
- (limited-support) multi-scale transform for global and local study
  - wavelet (and is isotropic 2D adaption) well-suited for 1D signal analysis
  - curvelet (anisotropic 2D decomposition) well-suited for 2D signals

Multi-scale, multi-orientation transformation with atoms indexed with a position parameter

$$\mathbf{f} = \sum_{j,k,l} \langle \mathbf{f}, \varphi_{j,l,k} \rangle \varphi_{j,l,k}$$

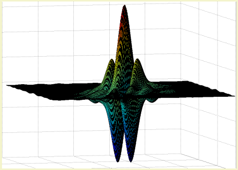

Curvelet atom $\varphi_{j,l,k}$

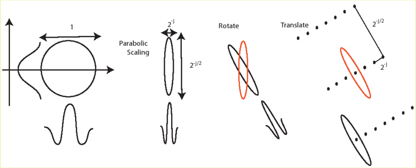

Scaling, rotations and translations

(E. J. Candès and D. L. Donoho, 2004), (L. Demanet 2006)

satellite images = IR radiation measured by satellites.
signals are well described in terms of frequential characteristics

- fourier transform for global study of the signal
- (limited-support) multi-scale transform for global and local study
  - wavelet (and is isotropic 2D adaption) well-suited for 1D signal analysis
  - curvelet (anisotropic 2D decomposition) well-suited for 2D signals

Curvelet transform is well adapted for signals with 2D discontinuities

Wavelets

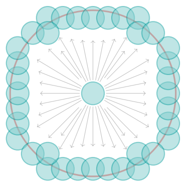

$$\|\mathbf{f} - \hat{\mathbf{f}}_m\| \approx m^{-1}$$

Curvelets

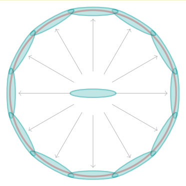

$$\|\mathbf{f} - \hat{\mathbf{f}}_m\| \approx Cm^{-2}(\log m)^3$$

(E. J. Candès and D. L. Donoho, 2004), (L. Demanet 2006)

satellite images = IR radiation measured by satellites.
signals are well described in terms of frequential characteristics

- fourier transform for global study of the signal
- (limited-support) multi-scale transform for global and local study
  - wavelet (and is isotropic 2D adaption) well-suited for 1D signal analysis
  - curvelet (anisotropic 2D decomposition) well-suited for 2D signals

- Pixel basis : spatial correlation may be difficult to take into account; adequate denoising functions and well modelled covariance matrices could achieve this(!)
- Multi-scale decompostions
  - spatial correlation is automatically managed by coarse scale elements
  - local effects are emphasized by fine scale elements

  adequate thresholding functions are used to reduce observation size ($\Rightarrow$ rapid convergence) whithout (necessarily) degrading the signal quality

Motivation : vortex motion in a rotating platform

J.-B. Flór (LEGI) and I. Eames, 2002

Coriolis Platform
LEGI, Grenoble

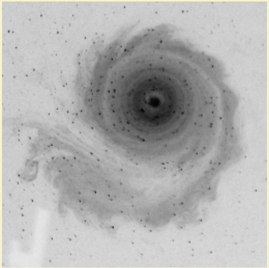

Simulation of an isolated vortex
in the atmosphere

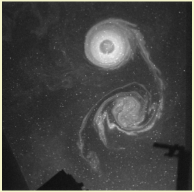

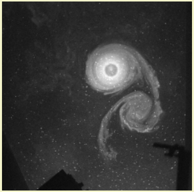

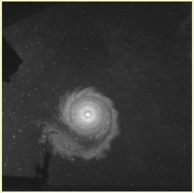

$\mathcal{E}_{\mathcal{F}\to\mathcal{S}}(\mathbf{f})$ = Threshold of the Curvelet Transform of the image $\mathbf{f}$

- Multi-scale, multi-orientation transformation with atoms indexed with a position parameter
- Decomposition : $\mathbf{f} = \sum_{j,k,l} \langle \mathbf{f}, \varphi_{j,l,k} \rangle \varphi_{j,l,k}$
- Threshold : $\mathcal{T}(\mathbf{f}) = \sum_{(j,k,l)\in E} \langle \mathbf{f}, \varphi_{j,l,k} \rangle \varphi_{j,l,k}$

$\mathcal{E}_{\mathcal{F}\to\mathcal{S}}(\mathbf{f})$ = Threshold of the Curvelet Transform of the image $\mathbf{f}$

- Multi-scale, multi-orientation transformation with atoms indexed with a position parameter
- Decomposition : $\mathbf{f} = \sum_{j,k,l} \langle \mathbf{f}, \varphi_{j,l,k} \rangle \varphi_{j,l,k}$
- Threshold : $\mathcal{T}(\mathbf{f}) = \sum_{(j,k,l)\in E} \langle \mathbf{f}, \varphi_{j,l,k} \rangle \varphi_{j,l,k}$
  - Fast Discrete Curvelet Transform (FDCT) implementations run in $O(n^2 \log n)$ for $n \times n$ cartesian arrays (`www.curvelet.org`) (C++, C++//, Matlab™)
  - Adjoint curvelet transform = inverse curvelet transform

Evolution of the state vector $x = (\mathbf{u}, \mathbf{v}, \mathbf{h})$: shallow-water model

$$\begin{cases} \partial_t u - u\partial_x u + v\partial_y u - fv + g\partial_x h + \mathcal{D}(u) & = & \mathcal{F}_u \\ \partial_t v + u\partial_x v + v\partial_y v + fu + g\partial_y h + \mathcal{D}(v) & = & \mathcal{F}_v \\ \partial_t h + \partial_x(hu) + \partial_y(hv) & = & 0 \end{cases}$$

Observation Operator

Tracer transport equation : (concentration $\mathbf{q}$) $\quad \partial_t \mathbf{q} + u\partial_x \mathbf{q} + v\partial_y \mathbf{q} - \nu_T \Delta \mathbf{q} = 0$

Syntetic Image Sequence : $\quad \mathcal{I}_{\mathcal{X}\to\mathcal{F}}[\mathbf{u}, \mathbf{v}, \mathbf{h}] = \mathbf{q}$

Observation Operator $\quad \mathcal{H}_{\mathcal{X}\to\mathcal{S}} = \mathcal{E}_{\mathcal{F}\to\mathcal{S}} \circ \mathcal{I}_{\mathcal{X}\to\mathcal{F}} = \mathcal{T}(\mathrm{FDCT}[\mathbf{q}])$

Cost function

$$J(X_0) = \alpha_o \int_0^T \|\mathcal{T}(FDCT[\mathbf{f}]) - \mathcal{T}(FDCT[\mathbf{q}])\|_{\mathcal{S}}^2 dt + \alpha_b \|X_0\|_{\mathcal{X}}^2, \quad \alpha_b \lll \alpha_o$$

Evolution of the state vector $x = (\mathbf{u}, \mathbf{v}, \mathbf{h})$: shallow-water model

$$\begin{cases} \partial_t u - u\partial_x u + v\partial_y u - fv + g\partial_x h + \mathcal{D}(u) & = & \mathcal{F}_u \\ \partial_t v + u\partial_x v + v\partial_y v + fu + g\partial_y h + \mathcal{D}(v) & = & \mathcal{F}_v \\ \partial_t h + \partial_x(hu) + \partial_y(hv) & = & 0 \end{cases}$$

Observation Operator

Tracer transport equation : (concentration $\mathbf{q}$) $\quad \partial_t \mathbf{q} + u\partial_x \mathbf{q} + v\partial_y \mathbf{q} - \nu_T \Delta \mathbf{q} = 0$

Syntetic Image Sequence : $\quad \mathcal{I}_{\mathcal{X}\to\mathcal{F}}[\mathbf{u}, \mathbf{v}, \mathbf{h}] = \mathbf{q}$

Observation Operator $\quad \mathcal{H}_{\mathcal{X}\to\mathcal{S}} = \mathcal{E}_{\mathcal{F}\to\mathcal{S}} \circ \mathcal{I}_{\mathcal{X}\to\mathcal{F}} = \mathcal{T}(\mathrm{FDCT}[\mathbf{q}])$

Cost function

$$J(X_0) = \alpha_o \int_0^T \|\mathcal{T}(FDCT[\mathbf{f}]) - \mathcal{T}(FDCT[\mathbf{q}])\|_{\mathcal{S}}^2 dt + \alpha_b \|X_0\|_{\mathcal{X}}^2, \quad \alpha_b \lll \alpha_o$$

Evolution of the state vector $x = (\mathbf{u}, \mathbf{v}, \mathbf{h})$: shallow-water model

$$\begin{cases} \partial_t u - u\partial_x u + v\partial_y u - fv + g\partial_x h + \mathcal{D}(u) & = & \mathcal{F}_u \\ \partial_t v + u\partial_x v + v\partial_y v + fu + g\partial_y h + \mathcal{D}(v) & = & \mathcal{F}_v \\ \partial_t h + \partial_x(hu) + \partial_y(hv) & = & 0 \end{cases}$$

Observation Operator

Tracer transport equation : (concentration $\mathbf{q}$) $\quad \partial_t \mathbf{q} + u\partial_x \mathbf{q} + v\partial_y \mathbf{q} - \nu_T \Delta \mathbf{q} = 0$

Syntetic Image Sequence : $\quad \mathcal{I}_{\mathcal{X}\to\mathcal{F}}[\mathbf{u}, \mathbf{v}, \mathbf{h}] = \mathbf{q}$

Observation Operator $\quad \mathcal{H}_{\mathcal{X}\to\mathcal{S}} = \mathcal{E}_{\mathcal{F}\to\mathcal{S}} \circ \mathcal{I}_{\mathcal{X}\to\mathcal{F}} = \mathcal{T}(\mathrm{FDCT}[\mathbf{q}])$

Cost function

$$J(X_0) = \alpha_o \int_0^T \|\mathcal{T}(FDCT[\mathbf{f}]) - \mathcal{T}(FDCT[\mathbf{q}])\|_{\mathcal{S}}^2 dt + \alpha_b \|X_0\|_{\mathcal{X}}^2, \quad \alpha_b \lll \alpha_o$$

Twin experiment

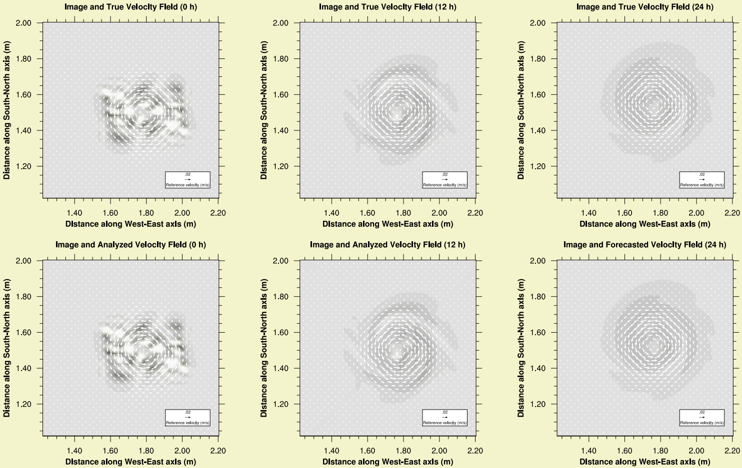

$t = 0\text{h}$ $t = 3\text{h}$ $t = 6\text{h}$

Error analysis

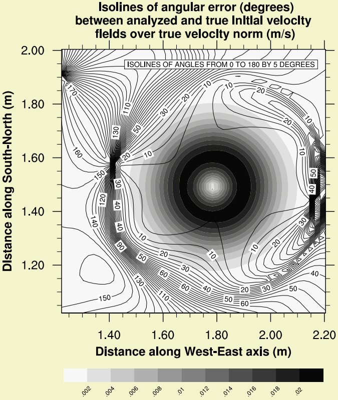

Barron angular error

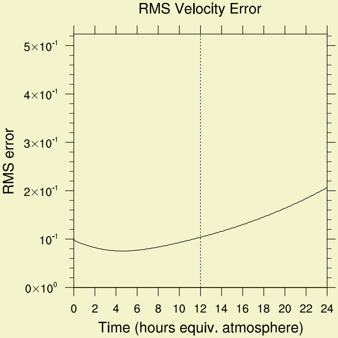

RMS error

Real images experiment

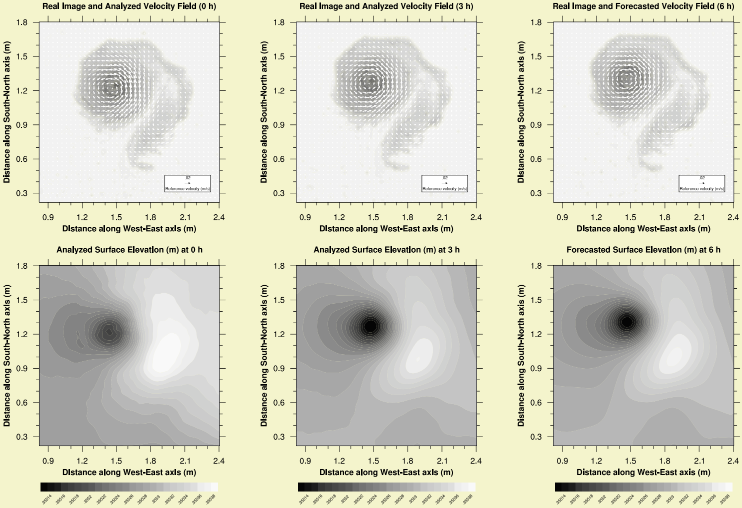

$t = 0\text{h}$ $t = 3\text{h}$ $t = 6\text{h}$

Images assimilation

I. Souopgui

Data Assimilation

Images

Assimilation of Image Sequences

Numerical Experiments

Description

Twin experiment

Real images experiment

Image operators

Conclusions

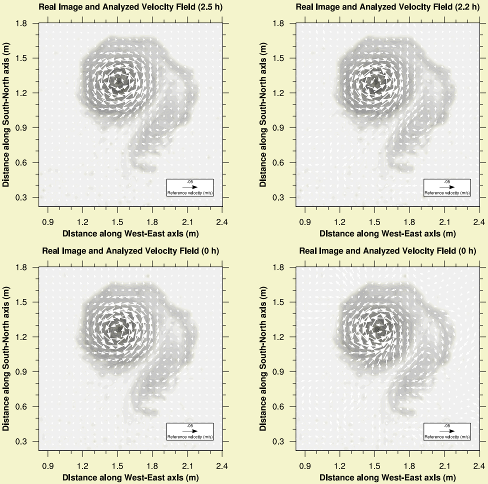

curvelet (600 ts) pixels (300 ts)

Thresholding

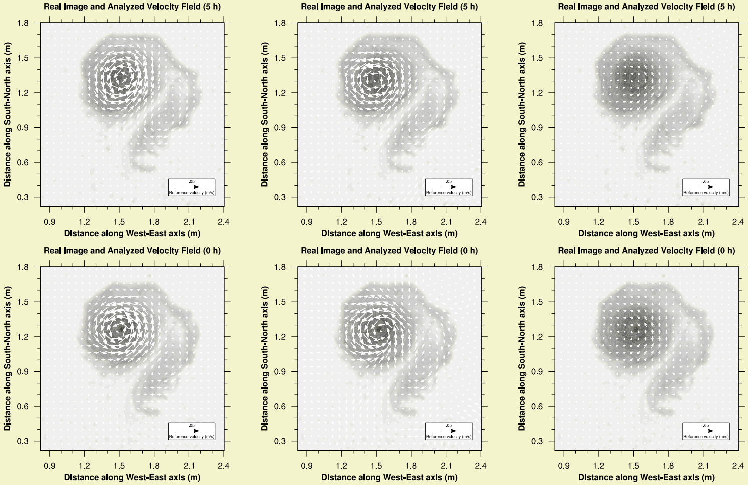

scale by scale zeroing coarse scale hard

Conclusions

- Image Sequences have a strong predictive potential but are still underused by numerical systems
- Pseudo observation techniques retrieve observations of state variables from images (estimated velocity fields)
- Direct Assimilation of Sequences of Images combines image-type information conistently with the underlying physical model
- DISA is based on high level images representation
- adequate threshold functions reduce obs size and ensure rapid convergence

Conclusions

- Image Sequences have a strong predictive potential but are still underused by numerical systems
- Pseudo observation techniques retrieve observations of state variables from images (estimated velocity fields)
- Direct Assimilation of Sequences of Images combines image-type information conistently with the underlying physical model
- DISA is based on high level images representation
- adequate threshold functions reduce obs size and ensure rapid convergence

Future works

- Comparison with pseudo-observation technique
- Analysis of threholding functions
- Going to more realistic problem